Full Paper

Journal of the Brazilian Chemical Society

https://dx.doi.org/10.21577/0103-5053.20260070

J. Braz. Chem. Soc. **2026**, *37-Spe1*, e-20260070, 1-11

Metabolomic Signatures of Alzheimer's Disease Patients Treated with a Cholinesterase Inhibitor

Mariana S. Marques,[a] *Micael D. L. Oliveira,*[a] *Thales F. D. Pereira,*[a] *Leda L. Talib,*[b] *Wagner F. Gattaz*[b] *and Alessandra Sussulini*[*,a,c]

[a]*Laboratório de Bioanalítica e Ciências Ômicas Integradas (LaBIOmics), Instituto de Química, Universidade Estadual de Campinas (UNICAMP), 13083-970 Campinas-SP, Brazil*

[b]*Laboratório de Neurociências (LIM 27), Instituto de Psiquiatria, Hospital das Clínicas da Faculdade de Medicina, Universidade de São Paulo (USP), 05403-903 São Paulo-SP, Brazil*

[c]*Instituto Nacional de Ciência e Tecnologia de Bioanalítica Lauro Kubota (INCTBio-LK), Instituto de Química, Universidade Estadual de Campinas (UNICAMP), 13083-970 Campinas-SP, Brazil*

Alzheimer's disease (AD) is a progressive neurodegenerative disorder for which acetylcholinesterase inhibitors (AChIs) are commonly prescribed to mitigate cognitive decline. In this study, untargeted metabolomics and lipidomics based on liquid chromatography coupled to high-resolution mass spectrometry (LC-HRMS) were applied to investigate metabolic alterations in plasma samples from AD patients before and during AChI treatment. Differential feature selection and pathway enrichment analyses revealed significant modulation of lipidic and energetic metabolism. Alterations in glycerophospholipid and glycosphingolipid metabolism, accompanied by a progressive reduction in phospholipids, suggest an increased demand for substrates associated with acetylcholine synthesis. Enrichment of carnitine transport and fat-soluble vitamin (E and D) metabolism after AChI treatment points to bioenergetic dysfunction and enhanced oxidative and inflammatory stress in AD. Changes in arginine and proline metabolism, carbohydrate metabolism, and butyrate metabolism further reflect key biochemical disturbances in AD, including glucose hypometabolism and nitrosative stress. These findings provide insights into the systemic metabolic effects of AChI therapy and highlight the potential of LC-HRMS-based metabolomics and lipidomics for biomarker discovery and therapeutic monitoring in AD.

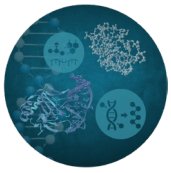

Keywords: Alzheimer's disease, cholinesterase inhibitor, metabolomics, lipidomics, liquid chromatography, mass spectrometry

Introduction

Alzheimer's disease (AD) is a terminal neurodegenerative disorder characterized by progressive memory loss, loss of cognitive ability, mood alterations, communication and reasoning problems, as well as an eventual inability to live independently.[1] The causes are still not completely elucidated, although some studies point to genetic predetermination.[2] There is no known cure for this disease, but some medications can delay symptom progression and improve the quality of life of the patients, acting mostly to reduce the effects of the symptoms.

The pathophysiological process of AD, or the preclinical phase, is hypothesized to begin before the onset of symptoms that could distinguish a phase of cognition considered normal from the senile state.[2] The main histopathological signature of AD is the presence of extracellular senile plaques derived from cleavage of the amyloid precursor protein (APP) and intercellular neurofibrillary entanglements formed by the hyperphosphorylation of the tau-protein.[3] Currently, in addition to the differential diagnosis performed, the criteria are fulfilled through anamnesis, classifying the disease as probable, possible, or definitive. For a definitive classification, a biopsy of cerebrospinal fluid or necropsy is required.[2]

To mitigate symptoms associated with AD, physicians frequently prescribe cholinesterase inhibitors as primary care.[4] These drugs mainly act by reducing the hydrolysis of the neurotransmitter acetylcholine (ACh) in the synaptic cleft. By preventing the enzyme acetylcholinesterase from

*e-mail: sussulini@unicamp.br
Editor handled this article: Andréa R. Chaves (Executive)
This publication is part of the special issue "Omics Sciences"

breaking down ACh, the drug increases the availability and duration of action of this neurotransmitter, thereby enhancing cholinergic transmission, which is critical for attention and memory.[4]

Metabolomics and lipidomics are bioanalytical approaches that enable the identification and/or quantification of various types of metabolites and lipids in biological systems, which can be used to develop new diagnostic and prognostic methods for diseases, as well as to discover novel biomarkers.[5] From studies in these omic levels, it has been possible to identify signatures of biological variations or disturbances in diseases such as cancer[6] and psychiatric disorders,[7] in addition to aiding advancements related to coronavirus disease (COVID-19) and the subsequent disorders caused by the disease.[8]

In omic studies investigating metabolic alterations associated with the pathophysiology of AD, glutamate dysregulation, as highlighted by Ashraf *et al.*,[9] is directly linked to disease progression and neuronal loss, which in turn may impair memory, cognition, and behavior.[9,10] Alterations in taurine and hypotaurine metabolism, as reported by Baloni *et al.*,[11] may also be related with AD pathology, but appear to primarily affect cognitive abilities.[11,12]

Regarding less polar metabolites, sphingolipids (lipids with bioactive roles, such as molecular signaling) were significantly reduced in AD patients, according to Huynh *et al*.[13] These molecules are not only essential components of cell membranes, but also participate in cellular processes such as growth, adhesion, differentiation, migration, and apoptosis.[14,15] Conversely, ceramides, found dysregulated in a murine model, act as precursors of sphingolipids and fatty acids in the lysosomal environment, yet exert neurotoxic effects when in excess.[16,17] This metabolic imbalance, although not completely elucidated, may provide important insights into the mechanisms of neurodegeneration in AD.[18]

Recent studies have also examined the role of the gut microbiome in cognitive decline, particularly alterations in fatty acids and in primary and secondary bile acids.[19] Gut health itself has been suggested as a potential factor in mitigating early neurodegenerative processes and cognitive decline in dementia.[20]

In this context, the present study aims to characterize the metabolomic and lipidomic profiles of plasma samples from AD patients before and after treatment with an acetylcholinesterase inhibitor (AChI), with the aim of identifying dysregulated pathways that may guide therapeutic strategies for symptom management. To achieve this, liquid chromatography coupled to high-resolution mass spectrometry (LC-HRMS) was employed as a state-of-the-art analytical platform for comprehensive metabolomic and lipidomic profiling. Chemometric and biostatistical approaches were subsequently applied to identify the biological pathways most strongly associated with both long-term AChI therapy and the natural course of AD progression.

Experimental

Exclusion criteria, demographic and clinical information

The exclusion criteria adopted prior to sample collection were: presence of sensorial or intellectual impairments that would prevent the adequate execution of the clinical tests; pre-existing clinical dementia; neurological diseases that may harm cognitive capacities; neurodegenerative diseases diagnosis, such as Parkinson's disease; clinical evidence of previous transient ischemic attack or stroke; unstable clinical condition or deteriorating health during initial evaluation; presence of major psychiatric disorders, such as schizophrenia or bipolar disorder; history or evidence of alcoholism or abuse of substances that are depressors of the central nervous system; recent or current use of anticholinergic drugs; refusal to sign the informed consent form.

The demographic and clinical data from the patients approved for research and subsequent follow-up are summarized in Table 1. The Cambridge Cognitive Examination (CAMCOG) was used to evaluate de evolution of the dementia state of the patients during research and it presented no significant alteration during the 6 months of data collection.

Table 1. Sample description and distribution of research participants (n = 23)

Variable	Mean (SD[a])
Gender	male: 8 female: 15
Age / years	75 (7)
CAMCOG[b] (t = 0 months)	57 (18)
CAMCOG[b] (t = 6 months)	59 (18)

[a]SD: standard deviation; [b]CAMCOG: Cambridge Cognitive Examination.

Sample collection

This study protocol was reviewed by the Ethics Committee of the University of São Paulo (USP), number 66092117.0.1001.0068. All study participants were previously informed of its purpose, and written consent was obtained. The participants of this study were recruited at the Geriatric Research Clinic of the Neuroscience Laboratory (LIM27) at the USP School of

Medical Sciences. Fifty-seven patients with a diagnosis of AD, according to the National Institute of Neurological and Communicative Disorders and Stroke - Alzheimer's Disease and Related Disorders Association (NINCDS-ADRDA) criteria, were recruited in the mild to moderate stage. In order to standardize the age range of the patients, those with ages outside the value of the standard deviation (SD) added to the mean were removed from the study, resulting in 23 patients who were followed up for each collection phase (before donepezil treatment, after 3 months of donepezil treatment, and after 6 months of donepezil treatment), totaling 69 samples.

40 mL of blood were collected in four 10 mL tubes containing sodium citrate anticoagulant at a concentration of 0.106 mol L^{-1}. To each tube, 1 mL of ACD-NH (a coagulant solution composed of glucose, citric acid, and sodium citrate) was added. The tubes were homogenized and centrifuged for 15 min at 1600 rpm and 20 ºC. Subsequently, the supernatants were transferred to a 50 mL Falcon tube, and the pH was adjusted to 6.5 using ACD-NH. The plasma was transferred to four polystyrene tubes and centrifuged for 10 min at 2400 rpm and 20 ºC. The supernatant was removed by inversion. Plasma aliquots were stored at −80 ºC in a freezer until analysis. Sample preparation and analysis were performed after thawing the plasma samples in an ice bath, following biosafety protocols for handling biological samples.

The samples in this study were divided into three groups:

(*i*) Twenty-three AD patients before donepezil treatment (AD);
(*ii*) The same twenty-three AD patients after 3 months of treatment with 5 mg of donepezil hydrochloride (AC1);
(*iii*) The same twenty-three AD patients after 3 months of treatment with 10 mg of donepezil hydrochloride (AC2).

Sample preparation

For the extractions using methyl *tert*-butyl ether (MTBE), following prior optimization, 40 µL of plasma were mixed with 300 µL of methanol and MTBE, thoroughly shaken and followed by the addition of a 0.1% (m/v) ammonium acetate solution before centrifugation for 15 min at 10 °C and rotation setting of 10000 g.[21] This leads to a triphasic separation of an organic phase on top, an aqueous phase in the middle, and a protein pellet in the bottom of the plastic tube. The extractions were carried out at room temperature. The aqueous and organic phases were dried using a centrifugal vacuum concentrator (SpeedVac, Eppendorf, Hamburg, Germany). In order to assess equipment stability, quality control (QC) samples, composed of a mixture of 15 µL of plasma from each sample and prepared in the same manner, were injected throughout the analysis batch.

LC-HRMS analyses

The organic and aqueous phases were reconstituted in 200 µL of the mobile phase referent to the start of the chromatographic run and analyzed in random order using an Ultimate 3000 LC (Thermo Fisher Scientific, Waltham, USA) system coupled to an Orbitrap QExactive (Thermo Fisher Scientific, Waltham, USA) mass spectrometer with a heated electrospray ionization (HESI) source in positive and negative modes. Full MS analysis (resolution: 70,000, *m/z* range 100-1500) was followed by sequential tandem mass spectrometry (MS/MS) analysis using data dependent acquisition (DDA) for the five most abundant peaks. Key parameters included a capillary voltage of 3.5 kV, drying gas flow of 10 L min^{-1} at 300 ºC, collision energy of 40 eV, autosampler at 10 ºC, and column oven at 45 ºC.

For lipidomics, the chromatographic gradient followed previous optimization[21] with a chromatographic flow rate of 150 µL min^{-1} and injection volume of 5 µL: mobile phase A consisted of acetonitrile:water (60:40 v/v) with 10 mmol L^{-1} ammonium acetate, while mobile phase B consisted of acetonitrile:isopropanol (10:90 v/v) with 10 mmol L^{-1} ammonium acetate. The employed gradient was: 0-2 min at 40% B, 3-6 min at 50% B, 6.1-8 min at 70% B, 9-11 min at 100% B, and 12-14 min for column stabilization with a 40% B gradient. The missing mentioned minutes represent linear ramps of gradient change.

For metabolomics, mobile phase A consisted of 0.1% (v/v) formic acid in water, while mobile phase B consisted of 0.1% (v/v) formic acid in acetonitrile. The gradient was: 0-1 min at 5% B, 1-3 min from 5 to 40% B, 3-13 min from 40 to 95% B, 13-18 min at 95% B, 18-1 min from 95 to 5% B, and 19-21 min at 5% B for column stabilization, with a chromatographic flow rate of 150 µL min^{-1} and injection volume of 5 µL. A Sigma-Aldrich Titan™ C18 column (1.9 µm particle size, 2.1 × 100 mm) was used for both analyses.

Data analysis

After the analysis of plasma samples from AD patients before and after treatment by LC-HRMS, the data were converted from .raw format to .mzML using the Proteowizard MSConverter software (version 3.0, Chambers, M.; MacLean, B.; MacCoss Lab, Tabb Lab, and Mallick Lab, 2008-2025). MS-DIAL[22] (version 4.9) was used for signal detection and spectrum alignment. Feature annotation was performed using the LipidBlast (version 2.4;

Kind, T.; Fiehn, O.; Fiehn Lab, University of California, 2013-2025) and MassBank of North America (MoNA) databases for lipidomics and metabolomics, respectively. In Tables S1 and S2, Supplementary Information (SI) section, the annotated lipids were manually named according to the LIPID MAPS classification.[23] Table S3 (SI section) describes the annotated metabolites and key parameters of data processing can be accessed in Tables S4 and S5 (SI section).

The adducts selected for lipidomics (negative mode) were: $[M - H]^-$, $[M + Na - 2H]^-$, $[M + Cl]^-$, $[M - 2H]^{2-}$, $[M + HAc - H]^-$, $[M - H_2O - H]^-$, $[M + CH_3COO]^-$, and $[M + HCOO]^-$. The adducts selected for lipidomics (positive mode) were: $[M + H]^+$, $[M + NH_4]^+$, $[M + CH_3OH + H]^+$, $[M + 2H]^{2+}$, $[M + ACN + H]^+$, $[M + Na]^+$, $[M + NH_4]^{2+}$, $[M + H - H_2O]^+$, $[M + ACN + H]^{2+}$, $[M + Na]^{2+}$, and $[M + H]^{2+}$. The adducts selected for metabolomics (positive mode) were: $[M + H]^+$, $[M + H - H_2O]^+$, $[M + CH_3OH + H]^+$, $[M + NH_4]^+$, $[M]^+$, $[M + Na]^+$, $[M + H - 2H_2O]^+$, $[M + 2H]^{2+}$, $[M + H - 2H_2O]^{2+}$, $[M + ACN + H]^+$, $[M + H - H_2O]^{2+}$, $[M + H]^{2+}$, $[M + 2ACN + H]^+$, $[M + ACN + Na]^+$, $[M + Na]^{2+}$, $[M + CH_3OH + H]^{2+}$, $[M - H_2O + H]^+$, and $[M + NH_4]^{2+}$. The adducts selected for metabolomics (negative mode) were: $[M - H]^-$, $[M - 2H]^{2-}$, $[M + HAc - H]^-$, $[M - H_2O - H]^-$, $[M + Na - 2H]^-$, and $[M + Cl]^-$.

One-way analysis of variance (ANOVA) was performed using the statistical analysis (one factor) functionality in the online software MetaboAnalyst[24] (version 6.0). The script for multivariate analysis was developed in Python 3.13.5 using the scikit-learn library[25] (version 1.7.2, developed by Pedregosa *et al.*[25]). Principal component analysis (PCA) and partial least squares discriminant analysis (PLS-DA) were applied using linear regression methods. The results were visualized using the Matplotlib library[26] (version 3.8.2, Matplotlib development team, 2012-2025), which was responsible for generating the plots.

Data pretreatment

After LC-HRMS data acquisition and previous to the feature selection and annotation, the peak area information was further used to process and normalize the dataset. Each metabolomics or lipidomics dataset requires a specific type of normalization; therefore, the obtained data were optimized individually.[27] The results of this optimization are presented in Table 2. The purpose of normalizing, transforming, and scaling the data is to ensure they are comparable and normally distributed.

Moreover, data filtering was performed by excluding features with a relative standard deviation (RSD) above 25% in the QC samples, calculated as the ratio between the standard deviation and the mean intensity of each feature. In the case of metabolomics data obtained in negative ionization mode, a better Gaussian distribution was achieved by normalizing the data before applying the filter, whereas for other data, normalization was performed first, followed by filtering. Although this second approach does not strictly follow the workflow presented by MetaboAnalyst, it allowed for better comparability of the data, as they were already on the same scale and normalized.

Table 2. Optimization of normalization, transformation, and scaling parameters for metabolomics and lipidomics results

Analysis	Ionization mode	Normalization	Transformation	Scaling
Metabolomics	+	group PQN	cubic root	interval
Metabolomics	–	quantile	cubic root	none
Lipidomics	+	quantile	none	none
Lipidomics	–	quantile	none	none

PQN: probability quotient normalization.

Quality control analysis

For this study, QC samples were used to assess the stability of the chromatographic runs throughout the batch analysis. Periodic QC injections were performed, which are expected to be clustered and preferably centered in the PCA scores plot. Observing Figure 1, it is possible to confirm that for both ionization modes, in lipidomics experiments, the QCs are satisfactorily overlapped and centered in relation to the other data, indicating acceptable instrumental stability. Regarding the metabolomics experiments (Figure 2), samples are centered in the second principal component (PC2), but present variations on the PC1, which could indicate both instrumental instability and a high heterogeneity in sample metabolomics characteristics, especially for the positive mode of ionization.

Results and Discussion

The aim of this study was to investigate metabolic alterations in plasma from AD patients before and during treatment with an acetylcholinesterase inhibitor using an untargeted LC-HRMS metabolomics and lipidomics approach. After data acquisition and preprocessing, a total of 595 features were detected in the negative metabolomics dataset, 3079 features were detected in the positive metabolomics dataset, 2668 features were detected in the negative lipidomics dataset and 7465 features in the lipidomics dataset.

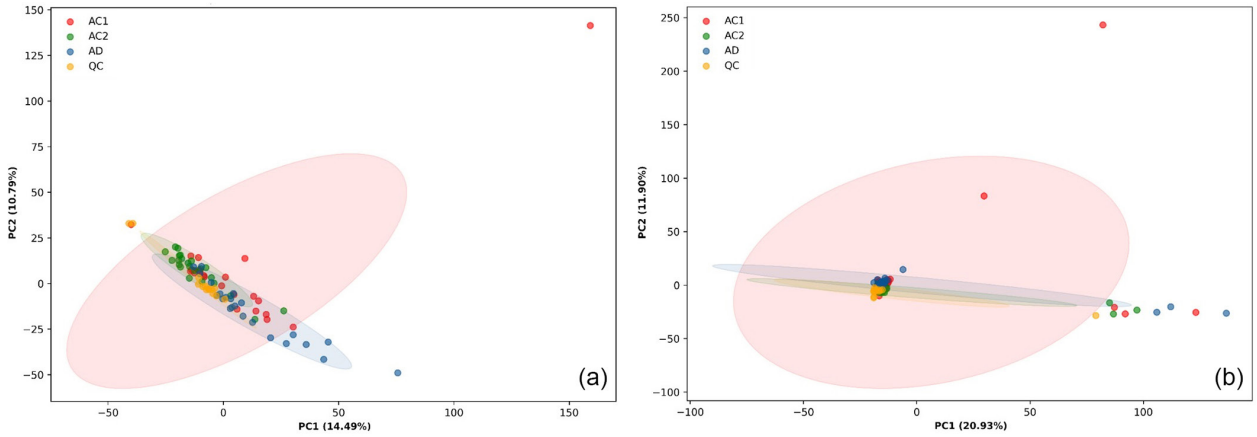

Figure 1. PCA scores plot from lipidomics data in ESI mode (a) positive and (b) negative. AD: AD patients before donepezil treatment; AC1: AD patients after 3 months of treatment with 5 mg of donepezil; AC2: AC1 patients after 3 additional months of treatment with 10 mg of donepezil; QC: quality control.

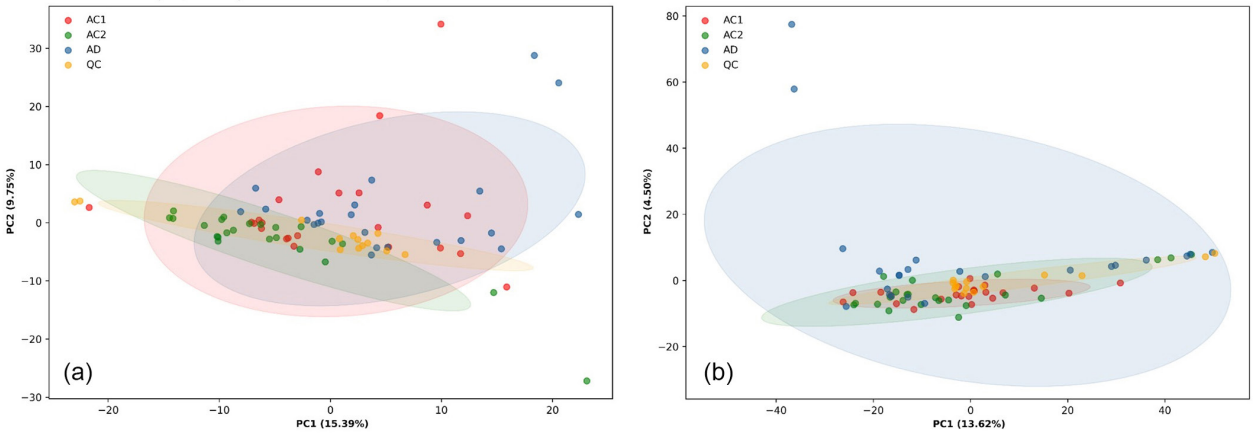

Figure 2. PCA scores plot from metabolomics data in ESI mode (a) positive and (b) negative. AD: AD patients before donepezil treatment; AC1: AD patients after 3 months of treatment with 5 mg of donepezil; AC2: AC1 patients after 3 additional months of treatment with 10 mg of donepezil; QC: quality control.

Selection of differential features

For the selection of differential features among the studied groups ANOVA was performed. From the resulting *p*-values, the selected features were those that presented a *p*-value lower than 0.05. The annotated differential metabolites are described in Tables S1 - S3 (SI section). The annotation of metabolites is essential for untargeted metabolomics and must follow a certain rigor. According to Schymanski *et al.*,[28] annotated metabolites are segregated in four types. For this study, most of the annotated metabolites fit in the criteria for level 2 identification, since they were annotated by comparison with database compounds.[28] Figure 3 presents a heatmap of the significantly altered metabolites and lipids and their relative concentration levels for AD, AC1, and AC2 groups.

A progressive reduction in phospholipids, such as PC 15:0_18:2, PG 9:0_16:0, and PI 9:0_20:5 was observed during AChI treatment (Figure 3c). Prolonged acetylcholinesterase activity due to enzymatic inhibition may intensify the need for synthesis, increasing precursor consumption and thereby reducing these phospholipid levels.[18] However, the biological significance of these changes in the present dataset remains unclear and may reflect broader metabolic adjustments.

Ceramides (Cer) are sphingolipids that, in AD, work not only as damage markers, but also as direct modulators of the amyloidogenic pathway that processes APP.[29] Studies in brain tissue and cerebrospinal fluid of patients presenting mild cognitive impairment, consistently show an increase in ceramides.[18] In Figures 3a and 3b, there is not a clear distinction between the intensities represented by the metabolites HexCer 16:2;O2/18:5;O, Cer 12:1;O3/12:0(2OH), Cer 20:0;O2/38:1(3OH) (FA 28:0), Cer 13:0;O2/32:5, HexCer 16:2;O3/16:4(2OH), Cer 13:0;O2/22:3;O, and Hex3Cer 16:1;O2/26:3 between AD and AC1 groups, but it is possible to observe a general decrease in these values when comparing the groups

AC1 and AC2. These variations may reflect metabolic adjustments during treatment; however, additional studies are necessary to determine whether these changes are directly associated with disease progression or therapeutic intervention.

N-Acylethanolamine (NAE) levels in Figure 3a presented a pattern with an initial rise under low drug dosage followed by a decrease after treatment intensification. NAEs have previously been associated with neuromodulatory processes and neuroinflammation: under low enzymatic inhibition, elevated NAE 18:0 may represent a compensatory mechanism to sustain cholinergic signaling, whereas higher acetylcholine availability at increased dosage reduces the need for such support.[30]

3-Indoxyl sulfate had its concentration level reduced after treatment with AChI (Figure 3c). This is a systemic toxic metabolite that promotes oxidative stress and apoptosis in neurons (differentiating SH-SY5Y cells), and its elevation is strongly correlated with cognitive impairment in patients with end-stage renal disease (ESRD) through mechanisms that induce cholinergic deficits and white matter damage.[31] However, the relevance of its variation in the context of Alzheimer's disease treatment remains unclear.

Arachidonic acid (AA), an omega-6 polyunsaturated fatty-acid (PUFA), is the central precursor for the synthesis of pro-inflammatory eicosanoids, including prostaglandins and leukotrienes and it is evident from the literature that the pathway of prostaglandin formation via archontate is activated in AD, an indicative of neuroinflammation.[32] PUFAs are vulnerable to lipoperoxidation, a process exacerbated by oxidative stress, an early characteristic of AD progression.[16] There is evidence that increased PUFA levels are associated with elevated iron-responsive element binding protein 2 (IREB2) in AD patients, but not in healthy controls, and that oxidized PUFAs drive cells toward ferroptosis.[9] This metabolite (Figure 3c) had its concentration level reduced after treatment with AChI.

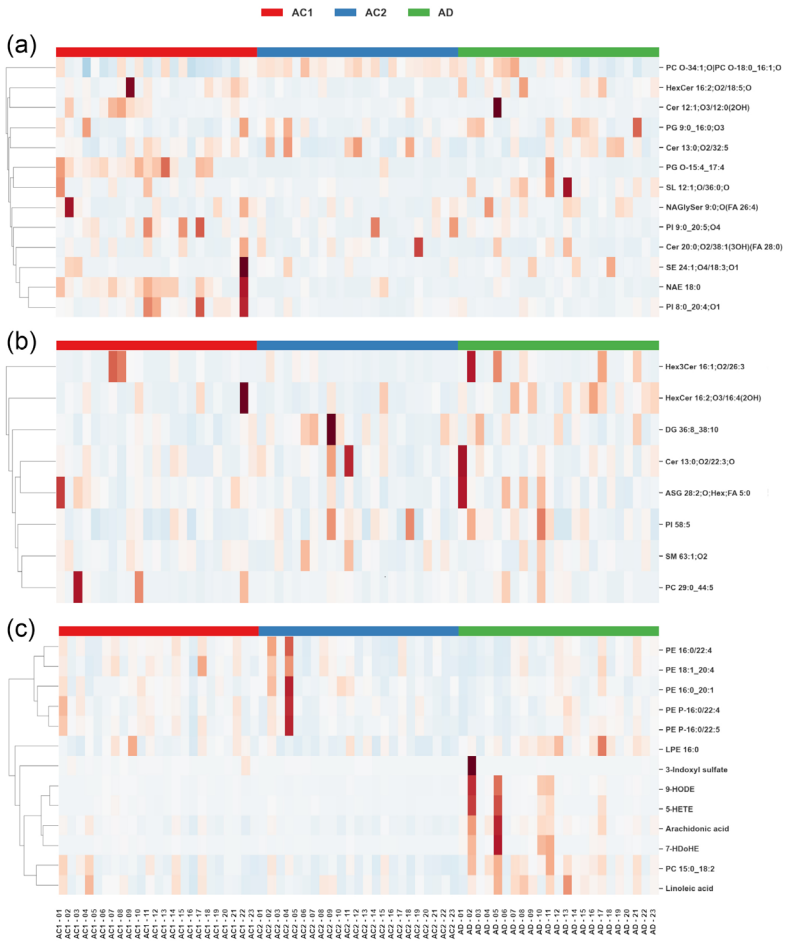

Figure 3. Heatmap of metabolites and lipids significantly altered among groups. Rows correspond to compounds and columns to individual samples. Red indicates relative increase and blue relative decrease in concentration levels (z-score normalized values). (a) Differential compounds obtained from lipidomics (negative mode) data, (b) differential compounds obtained from lipidomics (positive mode) data, (c) differential compounds obtained from metabolomics (negative mode) data. AD: AD patients before donepezil treatment; AC1: AD patients after 3 months of treatment with 5 mg of donepezil; AC2: AC1 patients after 3 additional months of treatment with 10 mg of donepezil.

The oxylipin 5-hydroxyeicosatetraenoic acid (5-HETE) presented reduced relative abundance after treatment (Figure 3c). 5-HETE is an eicosanoid derived from AA through enzymatic oxidation catalyzed by lipoxygenase (LOX). Donepezil has been reported to increase calcium-independent phospholipase A_2 ($iPLA_2$) activity, the enzyme responsible for cleaving phospholipids at the *sn*-2 position and releasing free fatty acids (including AA) that can subsequently enter LOX and cyclooxygenase (COX) oxidative pathways.[33]

7-Hydroxydocosahexaenoic acid (7-HdoHE) is an oxylipin derived from the oxidation of docosahexaenoic acid (DHA), an omega-3 PUFA, through the LOX pathway. The elevation of 7-HDoHE in states of frailty suggests an attempt from the organism to activate compensatory anti-inflammatory cascades or a failure to metabolize this compound using the 15-prostaglandin dehydrogenase (15-PGDH) enzyme.[34] Considering that elevated levels of 7-HDoHE correlate with the worsening of motor capabilities and frailty in a study conducted with elderly women, the reduction in the concentration of this metabolite (Figure 3c) may be a biochemical reflection of donepezil clinical efficacy in the stabilization of neurodegeneration.[35]

A relative decrease in linoleic acid (LA), another omega-6 PUFA, during AChI treatment was observed (Figure 3c). The observed reduction in its concentration level after treatment could indicate increased metabolic use of these lipids as part of neurochemical compensation, but more research is needed to further clarify the biological implications of such changes.

9-Hydroxyoctadecadienoic acid (9-HODE) is an oxylipin derived from oxidation of LA and serves mostly as a marker associated with vascular damage. There is also a negative association with the volume of grey matter, suggesting that the accumulation of this oxidized metabolite contributes to neurodegeneration and cerebral atrophy.[36] Since most of 9-HODE is partly originated from the non-enzymatic oxidation of LA via reactive oxygen species (ROS), donepezil property of reducing the production of free radicals directly reduces the conversion rates of LA into 9-HODE, which is consistent with the findings presented in Figure 3c.

Identified biochemical pathways

Metabolic pathways related to AD were identified through metabolomic and lipidomic analyses using Mummichog tools and a summarization of their impacts on the disease can be found in Figures 4 and 5 for lipidomics and metabolomics, respectively.[37]

The enrichment analysis of lipidomics data reveal alterations in the metabolism of sphingolipids, especially in the glycosphingolipid pathways of biosynthesis and metabolism, which are consistently enriched in the AD *vs.* AC1 and AC1 *vs.* AC2 comparisons (Figure 4). This finding is aligned to the literature, which describes AD as a condition marked by the accumulation of neurotoxic ceramides and the reduction of sphingomyelin and gangliosides, essential to synaptic integrity.[17] The increase of ceramides favors the stabilization of β-site amyloid precursor protein-cleaving enzyme 1 (BACE1) and increases the production of amyloid β (Aβ), while the decreased level of gangliosides compromises the organization of membrane lipid rafts and impairs APP

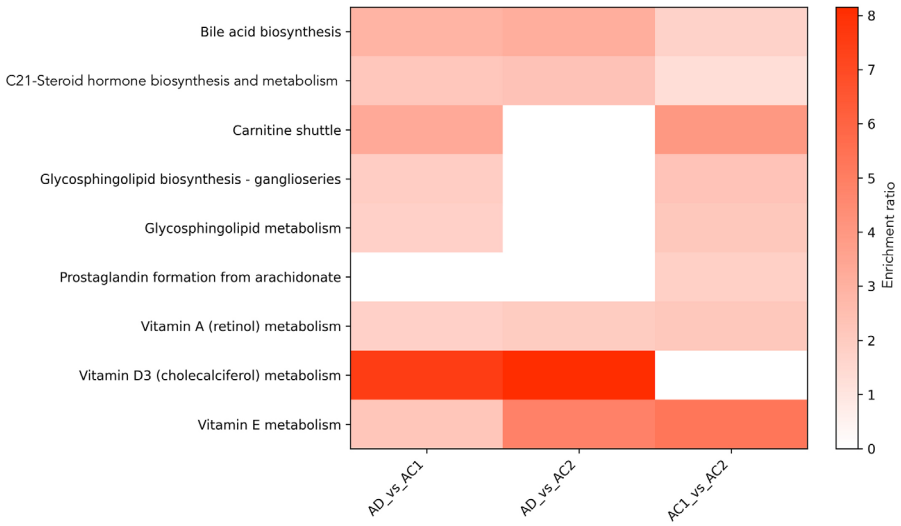

Figure 4. Pathway enrichment analysis of untargeted lipidomics data using Mummichog v1.0 with the lipid-focused pathway library. The heatmap summarizes enriched metabolic pathways across the three paired clinical conditions. Color intensity reflects the enrichment ratio, with darker red indicating stronger pathway enrichment. AD: AD patients before donepezil treatment; AC1: AD patients after 3 months of treatment with 5 mg of donepezil; AC2: AC1 patients after 3 additional months of treatment with 10 mg of donepezil.

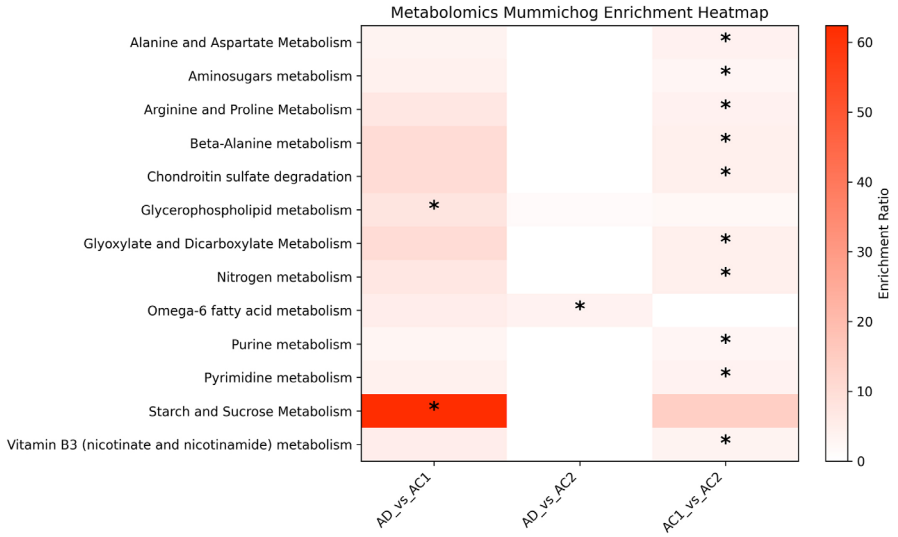

Figure 5. Pathway enrichment analysis of untargeted metabolomics data using Mummichog v2.0 with the Kyoto Encyclopedia of Genes and Genomes (KEGG) pathway library. The heatmap summarizes enriched metabolic pathways across the three paired clinical conditions. Color intensity reflects the enrichment ratio, with darker red indicating stronger pathway enrichment. Black asterisks highlight pathways that reached statistical significance after Mummichog permutation testing ($p < 0.05$). AD: AD patients before donepezil treatment; AC1: AD patients after 3 months of treatment with 5 mg of donepezil; AC2: AC1 patients after 3 additional months of treatment with 10 mg of donepezil.

traffic.[18] Therefore, the enriched pathways suggest that imbalance between ceramides and glycosphingolipids constitutes a central biochemical axis in the disease progression, being partially modulated by donepezil use.

The enrichment of the glycosphingolipid biosynthesis, ganglioseries pathway in Figure 4, point to a direct remodulation of gangliosides: molecules particularly abundant in neurons and that are crucial for differentiation, neuroplasticity and synaptogenesis.[17,18] The literature reports consistent reduction of monosialotetrahexosylganglioside (GM1); monosialotrihexosylganglioside (GM2); monosialodihexosylganglioside (GM3) in brain areas affected by AD, reflecting a decrease in the synthesis of those types of lipids and neuronal loss.[13] Since gangliosides modulate the activity of secretases and APP, their decrease favors the amyloidogenic pathway.[38]

The carnitine shuttle pathway, highlighted in Figure 4, suggests alterations in the transportation of long-chained fatty acids to the mitochondrial environment, essential step for the β-oxidation and synthesis of acetyl-CoA.[39] This compound is fundamental to the synthesis of acetylcholine and its deficiency may contribute to the cholinergic deficit, characteristic of AD.[40] The literature reports that the impairment of β-oxidation and mitochondrial function precede clinical symptoms, indicating that the neuronal energetic system is compromised since the early stages of the disease.[41] This pathway alteration in the present study is coherent with the higher demand of energy induced by AChI, which increases synaptic activity.[32]

Pathways related to the metabolism of vitamin E (tocopherols and tocotrienols) and vitamin D (Figure 4) also emerged as modulated in the lipidomic profiles.[42] Vitamin E, one of the main lipophilic antioxidants in the central nervous system, protects PUFA-rich membranes from lipid peroxidation, a process exacerbated by the presence of ceramides and alterations in glycerophospholipids. Vitamin D, in turn, exerts important anti-inflammatory, neuroprotective, and microglial-modulating effects, and influences calcium metabolism, which is often dysregulated in AD.[43]

The heatmap of altered pathways concerning metabolomics data in Figure 5, points to dynamic alterations in the glycerophospholipids metabolism, including phosphatidylcholines (PCs) and lysophosphatidylcholines and derivatives (LPCs). The progressive decrease of PCs and LPCs throughout pharmacological intervention may be attributed to an increased demand of cholinergic substrate, since PCs are precursors for the synthesis of acetylcholine.[44] The changed ratio of LPC to PC, described in other studies on the metabolism of AD, associated with the decreased activity of phospholipase A_2 (PLA_2) reinforces that scenario.[16]

Amongst the pathways concerning metabolomics results (Figure 5), the arginine and proline metabolism presented statistically significant enrichment, especially when comparing AC1 and AC2 patients, indicating an altered axis of the nitrogen metabolism. Arginine is substrate for the production of nitric oxide, whose dysregulation promotes nitrosative stress, excitotoxicity and neuronal damage: major elements of AD pathology. Excessive ammonia, one of the consequences of the dysfunction in the urea cycle, may activate the

nitric oxide/cyclic guanosine monophosphate signaling pathway (NO/cGMP) pathway and increase the formation of peroxinitrite, a highly cytotoxic chemical. The increase of the glutamate/γ-aminobutyric acid (GABA) ratio, frequently observed in AD patients, also relates to that pathway and contributes to excitotoxicity.[9,41]

The contribution of nitrogenated species to oxidative stress and inflammation is relevant in the structure of altered biochemical pathways: metabolomic studies have reported reduction of inosine and hypoxanthine in brain tissue of AD patients.[9]

Short-chain fatty acids such as butyrate have been implicated in gut-brain interactions and neuroinflammatory processes.[45] Alterations detected in the metabolomic profile may reflect either intestinal dysbiosis associated with the disease, as well as the interaction amongst systemic inflammation and brain dysfunction, which complements the landscape of oxidative stress and inflammation of AD.[46,47]

The carbohydrate metabolism pathway, including sugar and starch metabolism, presented statistically relevant alterations (Figure 5). Since glucose is the main energetic source of the central nervous system, its reduction compromises synaptic activity and favors the dependency of alternative routes such as β-oxidation and ketogenesis.[48,49] The perturbation of carbohydrates also affects the metabolism of amino acids such as glycine, serine, alanine and threonine, which influence neurotransmission, glutathione synthesis and upkeep of the cellular integrity.[6,20]

Conclusions

The present study employed untargeted metabolomics and lipidomics strategies using LC-HRMS to characterize metabolic signatures in plasma of AD patients before and during AChI treatment. Based on the annotated metabolites and lipids, especially phospholipids and sphingolipids, it was possible to better understand the potential metabolic pathways affected by AD and the use of acetylcholinesterase inhibitors. These results revealed dynamic modulation that suggests an interconnection between cholinergic treatment and lipidic/energetic metabolism.

Enrichment analyses highlighted the modulation of several metabolic pathways that are crucial in the pathophysiology of AD. In the lipidomics domain, alterations in glycosphingolipid metabolism and glycerophospholipid metabolism were observed, with a progressive reduction of phospholipids, indicating an intensified demand for substrates required for acetylcholine synthesis. Moreover, the enrichment of carnitine transport pathways and fat-soluble vitamin metabolism (E and D) suggests bioenergetic impairment and increased oxidative and inflammatory stress induced by the disease, which is partially modulated by enhanced synaptic activity under AChI treatment. With regard to the more polar metabolites, the arginine and proline metabolism pathways (nitrogen axis), carbohydrate metabolism (starch and sucrose), and butyrate metabolism presented statistically significant enrichment or contextual relevance. These alterations provide biochemical evidence for well-recognized dysfunctions in AD, such as cerebral glucose hypometabolism, nitrosative stress, and excitotoxicity. The identification of butyrate metabolism also reinforces the growing importance of the microbiota-gut-brain axis and its neuroprotective and anti-inflammatory effects in neurodegeneration.

In summary, the results obtained provide insights into the mechanism of action and systemic metabolic effects of donepezil in the plasma of AD patients. The identification of multiple altered metabolic and lipid pathways offers a promising perspective for the development of a biomarker panel after targeted studies for validation to support early detection and monitoring of disease progression, as well as to inform more effective therapeutic strategies aimed at directly modulating these biochemical alterations.

Supplementary Information

Supplementary information is available free of charge at http://jbcs.sbq.org.br as PDF file.

Data Availability Statement

The raw data is available at https://doi.org/10.25824/redu/TMEYU8[22] and the .py scripts are available at https://github.com/LaBIOmics-UNICAMP/Micael-statistics-toolkit

Acknowledgments

The authors thank the financial support of CNPq (306662/2022-1, 408338/2024-5) and FAPESP (2023/01800-2, 2025/26623-1). We also extend our gratitude to the patients, who are an integral part of this investigation, as well as the medical team of HC-FMUSP who collected the samples for this study.

Author Contributions

M. S. M.: data curation, formal analysis, investigation, methodology, software, validation, visualization, writing-original draft, writing (review and editing); M. D. L. O.: software, validation,

visualization, writing (review and editing); T. F. P. D.: visualization, writing (review and editing); L. L. T., W. F. G.: data curation, resources, writing (review and editing); A. S.: conceptualization, formal analysis, funding acquisition, project administration, resources, writing (review and editing).

References

1. Alzheimer's Association; *What is Alzheimer's Disease?* Department of Health and Human Services: Washington, DC, USA. [Link] accessed March 2026
2. Bateman, R. J.; Xiong, C.; Benzinger, T. L. S.; Fagan, A. M.; Goate, A.; Fox, N. C.; Marcus, D. S.; Cairns, N. J.; Xie, X.; Blazey, T. M.; Holtzman, D. M.; Santacruz, A.; Buckles, V.; Oliver, A.; Moulder, K.; Aisen, P. S.; Ghetti, B.; Klunk, W. E.; McDade, E.; Martins, R. N.; Masters, C. L.; Mayeux, R.; Ringman, J. M.; Rossor, M. N.; Schofield, P. R.; Sperling, R. A.; Salloway, S.; Morris, J. C.; *N. Engl. J. Med.* **2012**, *367*, 795. [Crossref]
3. Revett, T. J.; Baker, G. B.; Jhamandas, J.; Kar, S.; *J. Psychiatry Neurosci.* **2013**, *38*, 6. [Crossref]
4. Vecchio, I.; Sorrentino, L.; Paoletti, A.; Marra, R.; Arbitrio, M.; *J. Cent. Nerv. Syst. Dis.* **2021**, *13*, 1. [Crossref]
5. Rampler, E.; Abiead, Y. E.; Schoeny, H.; Rusz, M.; Hildebrand, F.; Fitz, V.; Koellensperger, G.; *Anal. Chem.* **2021**, *93*, 519. [Crossref]
6. Wishart, D. S.; *Nat. Rev. Drug Discovery* **2016**, *15*, 473. [Crossref]
7. Costa, A. C.; Riça, L. B.; van de Bilt, M.; Zandonadi, F. S.; Gattaz, W. F.; Talib, L. L.; Sussulini, A.; *Metabolites* **2023**, *13*, 600. [Crossref]
8. Hasan, M. R.; Suleiman, M.; Pérez-López, A.; *Front. Genet.* **2021**, *12*, 721556. [Crossref]
9. Ashraf, A.; Jeandriens, J.; Parkes, H. G.; So, P.-W.; *Redox Biol.* **2020**, *32*, 101494. [Crossref]
10. Altiné-Samey, R.; Antier, D.; Mavel, S.; Dufour-Rainfray, D.; Balageas, A.-C.; Beaufils, E.; Emond, P.; Foucault-Fruchard, L.; Chalon, S.; *Fundam. Clin. Pharmacol.* **2021**, *35*, 582. [Crossref]
11. Baloni, P.; Funk, C. C.; Yan, J.; Yurkovich, J. T.; Kueider-Paisley, A.; Nho, K.; Heinken, A.; Jia, W.; Mahmoudiandehkordi, S.; Louie, G.; Saykin, A. J.; Arnold, M.; Kastenmüller, G.; Griffiths, W. J.; Thiele, I.; Alzheimer's Disease Metabolomics Consortium; Kaddurah-Daouk, R.; Price, N. D.; *Cell Rep. Med.* **2020**, *1*, 100138. [Crossref]
12. Zhan, G.; Yang, N.; Li, S.; Huang, N.; Fang, X.; Zhang, J.; Zhu, B.; Yang, L.; Yang, C.; Luo, A.; *Aging* **2018**, *10*, 1257. [Crossref]
13. Huynh, K.; Lim, W. L. F.; Giles, C.; Jayawardana, K. S.; Salim, A.; Mellett, N. A.; Smith, A. A. T.; Olshansky, G.; Drew, B. G.; Chatterjee, P.; Martins, I.; Laws, S. M.; Bush, A. I.; Rowe, C. C.; Villemagne, V. L.; Ames, D.; Masters, C. L.; Arnold, M.; Nho, K.; Saykin, A. J.; Baillie, R.; Han, X.; Kaddurah-Daouk, R.; Martins, R. N.; Meikle, P. J.; *Nat. Commun.* **2020**, *11*, 5698. [Crossref]
14. Shen, S.; Yang, L.; Li, L.; Bai, Y.; Cai, C.; Liu, H.; *J. Chromatogr. B* **2017**, *1068*, 41. [Crossref]
15. Hannun, Y. A.; Obeid, L. M.; *Nat. Rev. Mol. Cell Biol.* **2018**, *19*, 175. [Crossref]
16. Zhang, X.; Liu, W.; Zan, J.; Wu, C.; Tan, W.; *Sci. Rep.* **2020**, *10*, 14509. [Crossref]
17. van Echten-Deckert, G.; Walter, J.; *Prog. Lipid Res.* **2012**, *51*, 378. [Crossref]
18. Haughey, N. J.; Bandaru, V. V. R.; Bae, M.; Mattson, M. P.; *Biochim. Biophys. Acta, Lipids Lipid Metab.* **2010**, *1801*, 878. [Crossref]
19. Wu, L.; Han, Y.; Zheng, Z.; Peng, G.; Liu, P.; Yue, S.; Zhu, S.; Chen, J.; Lv, H.; Shao, L.; Sheng, Y.; Wang, Y.; Li, L.; Li, L.; Wang, B.; *Nutrients* **2021**, *13*, 228. [Crossref]
20. Tran, T. T. T.; Corsini, S.; Kellingray, L.; Hegarty, C.; Le Gall, G.; Narbad, A.; Müller, M.; Tejera, N.; O'Toole, P. W.; Minihane, A.-M.; Vauzour, D.; *FASEB J.* **2019**, *33*, 8221. [Crossref]
21. Marques, M.; Ferreira, P.; Pereira, T.; Sussulini, A.; *Br. J. Anal. Chem.* **2023**, *40*, 99. [Crossref]
22. Tsugawa, H.; Ikeda, K.; Takahashi, M.; Satoh, A.; Mori, Y.; Uchino, H.; Okahashi, N.; Yamada, Y.; Tada, I.; Bonini, P.; Higashi, Y.; Okazaki, Y.; Zhou, Z.; Zhu, Z.-J.; Koelmel, J.; Cajka, T.; Fiehn, O.; Saito, K.; Arita, M.; *Nat. Biotechnol.* **2020**, *38*, 1159. [Crossref]
23. Liebisch, G.; Fahy, E.; Aoki, J.; Dennis, E. A.; Durand, T.; Ejsing, C. S.; Fedorova, M.; Feussner, I.; Griffiths, W. J.; Köfeler, H.; Merrill, A. H.; Murphy, R. C.; O'Donnell, V. B.; Oskolkova, O.; Subramaniam, S.; Wakelam, M. J. O.; Spener, F.; *J. Lipid Res.* **2020**, *61*, 1539. [Crossref]
24. Pang, Z.; Lu, Y.; Zhou, G.; Hui, F.; Xu, L.; Viau, C.; Spigelman, A. F.; MacDonald, P. E.; Wishart, D. S.; Li, S.; Xia, J.; *Nucleic Acids Res.* **2024**, *52*, W398. [Crossref]
25. Pedregosa, F.; Varoquaux, G.; Gramfort, A.; Michel, V.; Thirion, B.; Grisel, O.; Blondel, M.; Prettenhofer, P.; Weiss, R.; Dubourg, V.; Vanderplas, J.; Passos, A.; Cournapeau, D.; Brucher, M.; Perrot, M.; Duchesnay, É.; *J. Mach. Learn. Res.* **2011**, *12*, 2825. [Crossref]
26. Hunter, J. D.; *Comput. Sci. Eng.* **2007**, *9*, 90. [Crossref]
27. Chong, J.; Wishart, D. S.; Xia, J.; *Curr. Protoc. Bioinf.* **2019**, *68*, e86. [Crossref]
28. Schymanski, E. L.; Jeon, J.; Gulde, R.; Fenner, K.; Ruff, M.; Singer, H. P.; Hollender, J.; *Environ. Sci. Technol.* **2014**, *48*, 2097. [Crossref]
29. Costantini, C.; Ko, M. H.; Jonas, M. C.; Puglielli, L.; *Biochem. J.* **2007**, *407*, 383. [Crossref]
30. Masuoka, T.; Uwada, J.; Kudo, M.; Yoshiki, H.; Yamashita, Y.; Taniguchi, T.; Nishio, M.; Ishibashi, T.; Muramatsu, I.; *Neuroscience* **2019**, *404*, 39. [Crossref]
31. Hsieh, C.-C.; Lu, K.-C.; Huang, C.-L.; Wang, J.-J.; Yeh, T.-Y.; Lin, S.-M.; Chung, Y.-L.; Hou, Y.-C.; Huang, Y.-S.; *Int. J. Med. Sci.* **2025**, *22*, 1736. [Crossref]

32. Talib, L. L.: *Biomarkers in Alzheimer's Disease: GSK3B and PLA2 in Response to Cholinesterase Inhibitors*; PhD Thesis, University of São Paulo, São Paulo, Brazil, 2014. [Link] accessed in April 2026
33. Siddiqui, A.; Akhtar, S.; Shah, Z.; Othman, I.; Kumari, Y.; *Curr. Neuropharmacol.* **2020**, *19*, 885. [Crossref]
34. Shinto, L. H.; Raber, J.; Mishra, A.; Roese, N.; Silbert, L. C.; *Metabolites* **2022**, *12*, 826. [Crossref]
35. Sepúlveda, M.; Palomo, I.; Montecino-Garrido, H.; Wehinger, S.; Rodriguez-Mañas, L.; Trostchansky, A.; Fuentes, E.; *Free Radicals Biol. Med.* **2024**, *223*, 160. [Crossref]
36. Shinto, L.; Lahna, D.; Murchison, C. F.; Dodge, H.; Hagen, K.; David, J.; Kaye, J.; Quinn, J. F.; Wall, R.; Silbert, L. C.; *J. Alzheimer's Dis.* **2020**, *74*, 65. [Crossref]
37. Li, S.; Park, Y.; Duraisingham, S.; Strobel, F. H.; Khan, N.; Soltow, Q. A.; Jones, D. P.; Pulendran, B.; *PLoS Comput. Biol.* **2013**, *9*, e1003123. [Crossref]
38. Kakio, A.; Nishimoto, S.; Yanagisawa, K.; Kozutsumi, Y.; Matsuzaki, K.; *Biochemistry* **2002**, *41*, 7385. [Crossref]
39. Ameen, A. O.; Freude, K.; Aldana, B. I.; *Biomedicines* **2022**, *10*, 2778. [Crossref]
40. Villeda-González, J. D.; Gómez-Olivares, J. L.; Baiza-Gutman, L. A.; *J. Cell. Physiol.* **2024**, *239*, e31274. [Crossref]
41. Ardanaz, C. G.; Ramírez, M. J.; Solas, M.; *Int. J. Mol. Sci.* **2022**, *23*, 3785. [Crossref]
42. Mangialasche, F.; Solomon, A.; Kåreholt, I.; Hooshmand, B.; Cecchetti, R.; Fratiglioni, L.; Soininen, H.; Laatikainen, T.; Mecocci, P.; Kivipelto, M.; *Exp. Gerontol.* **2013**, *48*, 1428. [Crossref]
43. Mokry, L. E.; Ross, S.; Morris, J. A.; Manousaki, D.; Forgetta, V.; Richards, J. B.; *Neurology* **2016**, *87*, 2567. [Crossref]
44. Asghar, A.; Yousuf, M.; Fareed, G.; Nazir, R.; Hassan, A.; Maalik, A.; Noor, T.; Iqbal, N.; Rasheed, L.; *RSC Adv.* **2020**, *10*, 19346. [Crossref]
45. Senarath, R. M. U. S.; Oikari, L. E.; Bharadwaj, P.; Jayasena, V.; Martins, R. N.; Fernando, W. M. A. D. B.; *Nutrients* **2025**, *17*, 2286. [Crossref]
46. Bourassa, M. W.; Alim, I.; Bultman, S. J.; Ratan, R. R.; *Neurosci. Lett.* **2016**, *625*, 56. [Crossref]
47. El-Gharbawy, A.; Vockley, J.; *Pediatr. Clin. North Am.* **2018**, *65*, 317. [Crossref]
48. Ding, F.; Yao, J.; Rettberg, J. R.; Chen, S.; Brinton, R. D.; *PLoS One* **2013**, *8*, e79977. [Crossref]
49. Mett, J.; *Antioxidants* **2021**, *10*, 1991. [Crossref]

Submitted: December 15, 2025
Final version online: April 24, 2026